Supplementary figures and tables

Table S1: Complete genotypes and *n* for all experiments

MAIN FIGURES	GENOTYPE	NO. OF EXPERIMENTS
1A	*pebbled-gal4, UAS-opGCaMP6f* (X)	1
1B, 1C, 1D		3 (0.5% CO_2) 6 (1.25% CO_2) 9 (2.5% CO_2) 9 (5% CO_2) 9 (10% CO_2) 3 (15% CO_2
1D, 1E, 1F, 1G		4
2A	*pebbled-gal4, UAS-opGCaMP6f* (X)	1
2B, 2C		7
2D		4
3A, 3B	*or42b-gal4*/*UAS-DTI* (II); *orco-lexA, lexAop-opGCaMP6f* (III)	4-6 (SSR) 3-5 (calcium imaging)
3Ci	+/ *UAS-DTI* (II); o*r92a-gal4*/*orco-lexA, lexAop-opGCaMP6f* (III)	n/a
3Cii, 3Ciii	**ab1B ablated:** +/ *UAS-DTI* (II); o*r92a-gal4*/*orco-lexA, lexAop-opGCaMP6f* (III) **control:** SM6/+; o*r92a-gal4*/*orco-lexA, lexAop-opGCaMP6f* (III)	4 (ab1B ablated) 7 (control)
3Di	*pebbled-gal4, UAS-opGCaMP6f* (X); ; *orco-lexA/lexAop-DTI*	n/a
3Dii, 3Diii	***orco*+ ORNs ablated:** *pebbled-gal4, UAS-opGCaMP6f* (X); ;*orco-lexA/lexAop-DTI* **control:** *pebbled-gal4, UAS-opGCaMP6f* (X); ; +/ *lexAop-DTI*	3 (*orco*+ ORNs ablated) 7 (control)
4A	*pebbled-gal4, UAS-opGCaMP6f* (X); ; $orco^2$	n/a
4Bi, Bii	***orco*$^{+/-}$:** *pebbled-gal4, UAS-opGCaMP6f* (X); ; $orco^2$/MKRS ***orco*$^{-/-}$:** *pebbled-gal4, UAS-opGCaMP6f* (X); ; $orco^2$	4 ($orco^{+/-}$) *7* ($orco^{-/-}$)
4C	*pebbled-gal4, UAS-opGCaMP6f* (X); ; $gr63a^1$	n/a
4Di, Dii	***gr63a*$^{+/-}$:** *pebbled-gal4, UAS-opGCaMP6f* (X); ; $gr63a^1$/MKRS ***gr63a*$^{-/-}$:** *pebbled-gal4, UAS-opGCaMP6f* (X); ; $gr63a^1$	6 ($gr63a^{+/-}$) *7* ($gr63a^{-/-}$)
4E, 4Fi, 4Fii, 4G	*UAS-CsChrimson-mVenus*/SM6; *gr21a-gal4*/*orco-lexA, lexAop-opGCaMP6f*	4-5 (ATR) 5 (no ATR)
5A, 5B	+/ *UAS-DTI* (II); o*r92a-gal4*/*orco-lexA, lexAop-opGCaMP6f* (III)	3 (SSR) 4-11 (calcium imaging)
5C, 5D	*pebbled-gal4, UAS-opGCaMP6f* (X); $or42b^{EY14886}$ (II)	3 (SSR) 6-13 (calcium imaging)
5E, 5F	*pebbled-gal4, UAS-opGCaMP6f* (X); ; $orco^2$	3 (SSR) 3-5 (calcium imaging)
6A, 6B, 6C, 6D	**ORN:** *pebbled-gal4, UAS-opGCaMP6f* (X)	4 (ORN)

	PN: *GH146-gal4* (II); *UAS-opGCaMP6f* (III)	5-7 (PN)
6E	**ORN:** *pebbled-gal4, UAS-opGCaMP6f* (X) **VA2 PN:** *GH146-gal4* (II); *UAS-opGCaMP6f* (III) **V PN:** *VT12760-gal4*/*UAS-opGCaMP6f* (III)	4 (ORN) 5-7 (VA2 PN) 5 (V PN)
SUPPLEMENTARY FIGURES		
S1	n/a	n/a
S2A	*pebbled-gal4, UAS-opGCaMP6f* (X)	4
S2B	*pebbled-gal4, UAS-opGCaMP6f* (X)	8
S3A, S3B	*or42b-gal4*/ *UAS-DTI* (II); *orco-lexA, lexAop-opGCaMP6f* (III)	1
S4A	**ORN:** *pebbled-gal4, UAS-opGCaMP6f* (X) **PN:** *VT12760-gal4*/*UAS-opGCaMP6f* (III)	4 (ORN) 4 (PN)
S4B	*pebbled-gal4, UAS-opGCaMP6f* (X)	2
S4C	**control:** *+/Y;;orco-lexA, lexAop-opGCaMP6f* /+ ***shakB*^{2}/Y:** *shakB*^{2}/Y; ; *orco-lexA, lexAop-opGCaMP6f* (III)/+	2 (control) 4 (*shakB*^{2}/Y)
S4D	*pebbled-gal4, UAS-opGCaMP6f* (X)	3
S5A, S5B	*pebbled-gal4, UAS-opGCaMP6f* (X); *or42b*^{EY14886}/CyO	2
S5C, S5D	*pebbled-gal4, UAS-opGCaMP6f* (X); *or42b*^{EY14886}	2
S5E, S5F	**ab1A ablated:** *or42b-gal4*/ *UAS-DTI* (II); *orco-lexA, lexAop-opGCaMP6f* (III) ***or42b*$^{-/-}$:** *pebbled-gal4, UAS-opGCaMP6f* (X); *or42b*^{EY14886} (II)	3-4 (ab1A ablated) 6-13 (*or42b*$^{-/-}$)
S5G, S5H	*or42b-gal4*, *or42b*^{EY14886} (II); *UAS-opGCaMP6f* (III)	3
S6A, S6B, S6C, S6D	**ORN:** *pebbled-gal4, UAS-opGCaMP6f* (X) **PN:** *GH146-gal4* (II); *UAS-opGCaMP6f* (III)	4 (ORNs) 7 (PNs)

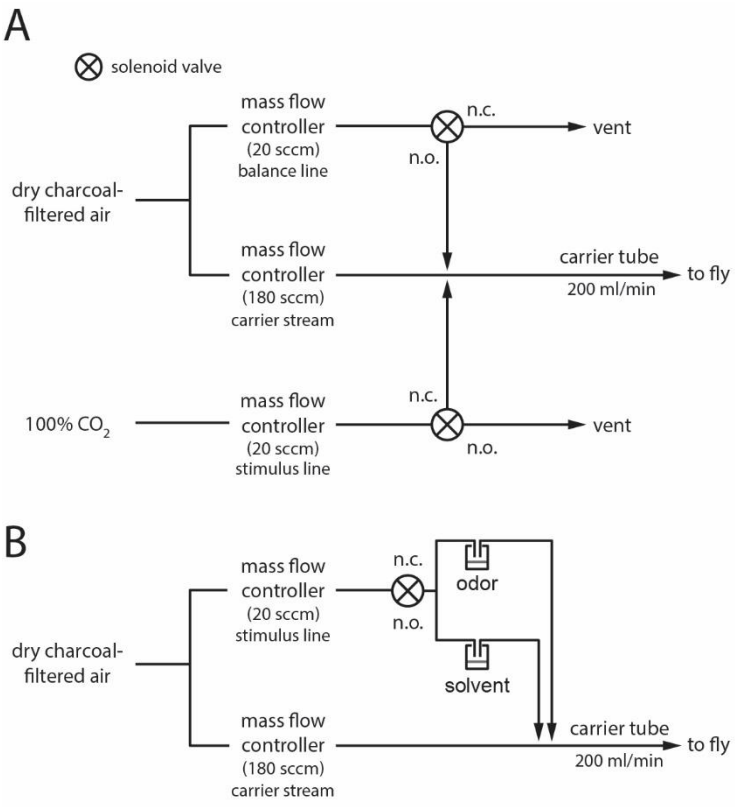

Figure S1: Odor delivery (related to Figure 1). A) Olfactometer design for delivery of 10% CO_2 stimulus. The flow rates of the stimulus and balance lines were always kept equal. The normally open (n.o.) outlet of each solenoid valve is open when the valve is unpowered and is closed when the valve is powered. The normally closed (n.c.) outlet of each solenoid valve is closed when the valve is unpowered and is open when the valve is powered. The same command signal is provided simultaneously to both valves. CO_2 stimuli of varying concentration were generated by adjusting the relative flow rates of the carrier line, and the stimulus and balance lines. For instance, for a 5% CO_2 stimulus, the mass flow controller for the carrier line was set to 190 sccm, and the stimulus and balance lines were set to 10 sccm. A total flow rate of 200 ml/min at the fly was used for all experiments, except for the optogenetic experiments in Figure 4E-G and the experiments in Figure 6, where a total flow rate of 2 L/min was used. B) Olfactometer design for delivery of all other odor stimuli besides CO_2 (see Methods). Odor concentrations in the figures and text are reported as the v/v dilution of the odor in solvent in the vial. Odors were diluted 10-fold in air compared to their concentration in the headspace of the vial. The only exceptions to this were acetic acid, which was always diluted 2-fold, and ammonia, which was diluted 100-fold in Figure 1, in air. Diagram is not drawn to scale.

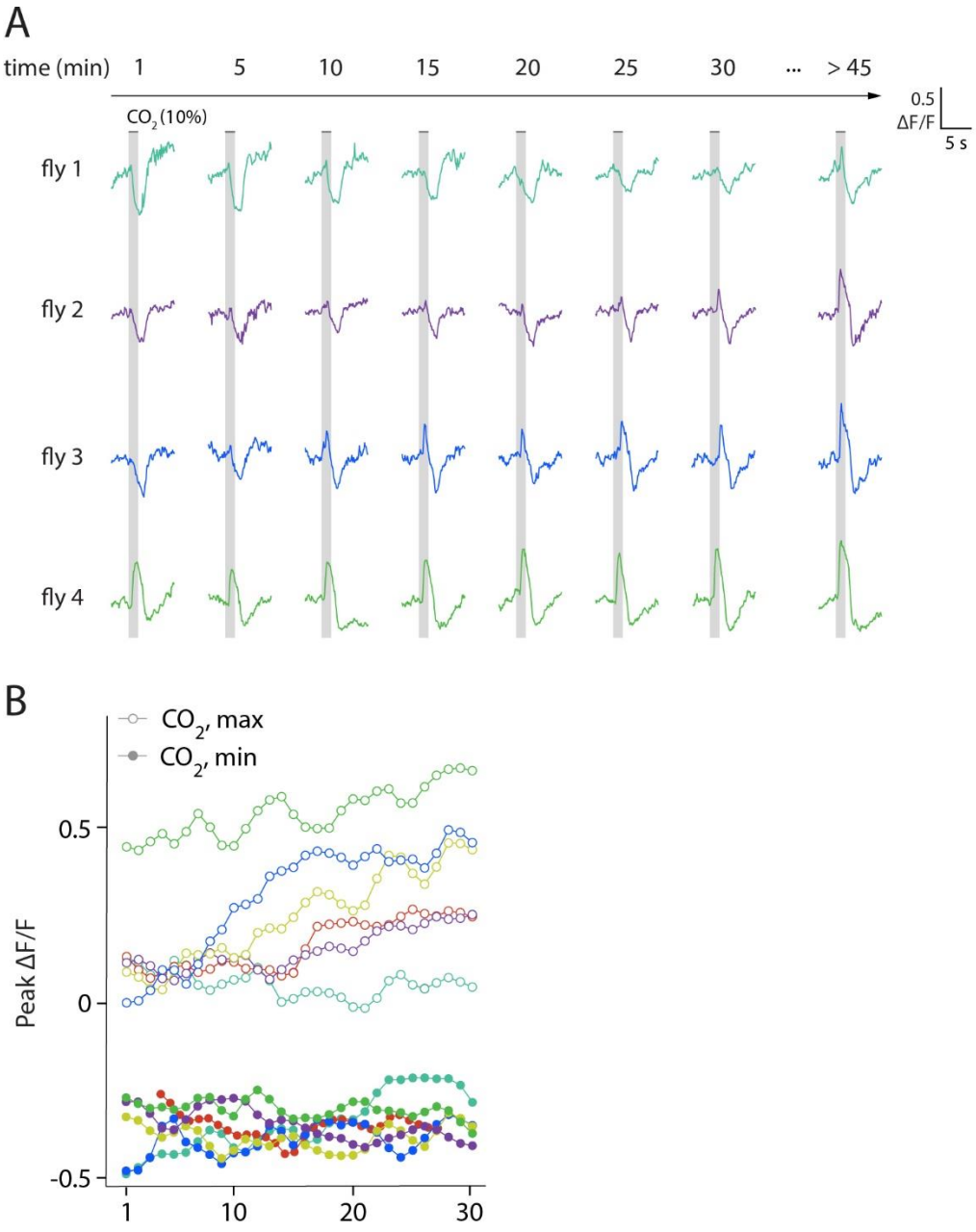

Figure S2: Variation in the time course of modulation of CO_2 responses in ORN terminals in VA2 from a low to high state (related to Figure 2). A) Single trial recordings of the change in fluorescence in ORN terminals in VA2 elicited by CO_2 over the duration of an experiment in four individual flies. A 3 s pulse of 10% CO2 was presented once every minute for 30 presentations; every fifth trial is shown. The fly was then left unstimulated on the rig, and a final measurement was taken between 45-60 min from the start of the experiment. B) Peak amplitudes of single-trial responses to CO_2 in ORN terminals in VA2, measured as in A, for six representative flies (which include the four in A). Both maximum peaks (open symbol) and minimum peaks (closed symbol) are shown. Note the variation in the time course of modulation of the CO_2 response across different experiments. During the 30-minute recording period, the recording began with responses to CO_2 in ORN terminals in VA2 already in the "high state" for one fly (fly 4, green), the response was mostly unchanged for one fly (fly 1, teal), and the CO_2 responses in the remaining four flies were significantly modulated over the course of the recordings, though at varying rates.

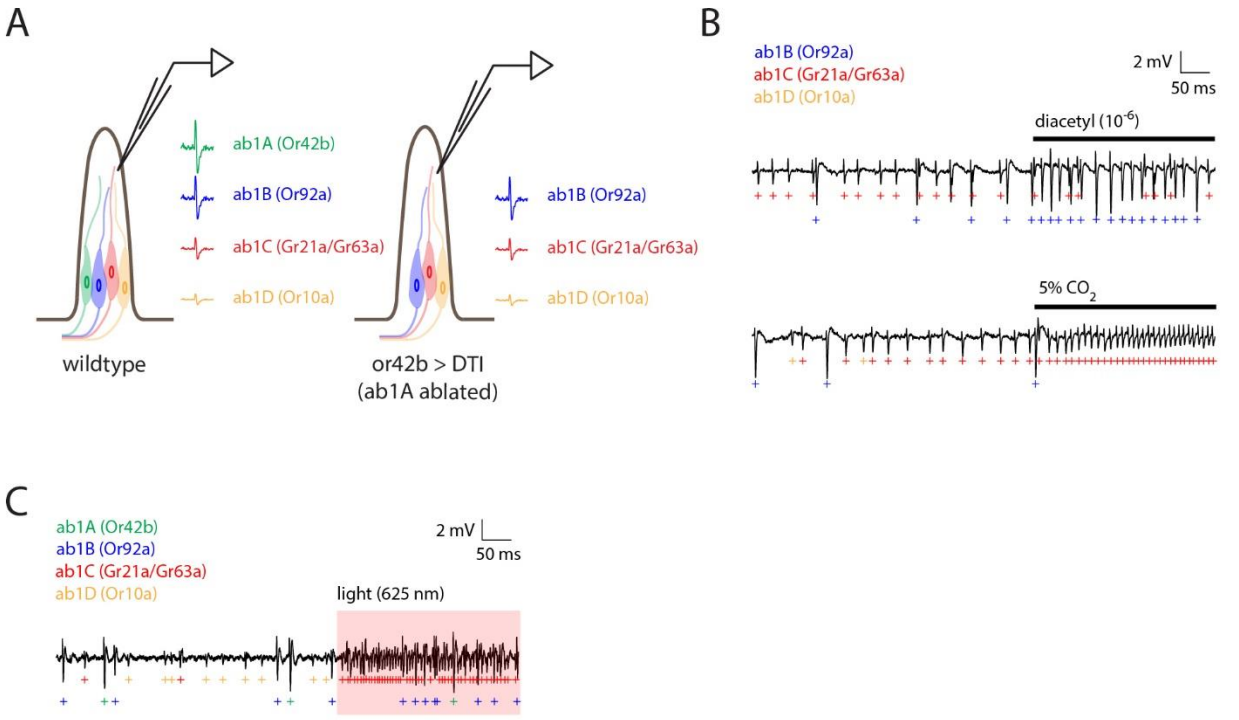

Figure S3: CO2 elicits spiking responses in ab1C, but not ab1B, ORNs (related to Figures 3 and 4). A) Schematic of experimental setup. The wildtype ab1 sensillum (left) houses four classes of ORNs – ab1A, ab1B, ab1C, and ab1D – which have characteristic spike amplitudes of descending size in extracellular single sensillum recordings (SSR). The two largest spikes, originating from the ab1A and ab1B, have the most similar amplitudes and are sometimes challenging to accurately assign to their respective ORN class, whereas spikes for the remaining two ORN classes, ab1C and ab1D, are easily identifiable and reliably sorted to their respective ORN class. To unambiguously identify ab1B spikes, we genetically ablated ab1A ORNs by expressing diphtheria toxin under the control of the or42b-gal4 driver (right). When ab1A was absent, ab1B spikes were easily differentiated from ab1C and ab1D spikes based on shape and amplitude. Note that, in this fly, GCaMP6f was also expressed in most ORNs under the control of orco-gal4 to allow imaging of calcium signals in ORN terminals in the same fly (Figure 3). B) Example SSR recordings from the ab1 sensillum in flies in which ab1A ORNs were ablated (panel A, right), showing the spiking responses of ab1B ORNs to 10^{-6} diacetyl (top) and the spiking responses of ab1C ORNs to 5% CO_2 (bottom). Note that no ab1B spikes (blue) were evoked when flies were presented with CO_2. C) Example SSR recording from the ab1 sensillum in flies expressing CsChrimson under the control of gr21a-gal4 and GCaMP6f under the control of orco-gal4 (see Figure 4E). Exposing the antenna to red light (625 nm, red shading) elicits spiking selectively in ab1C ORNs. "+" symbols mark identified spikes from each ORN class in the ab1 sensillum.

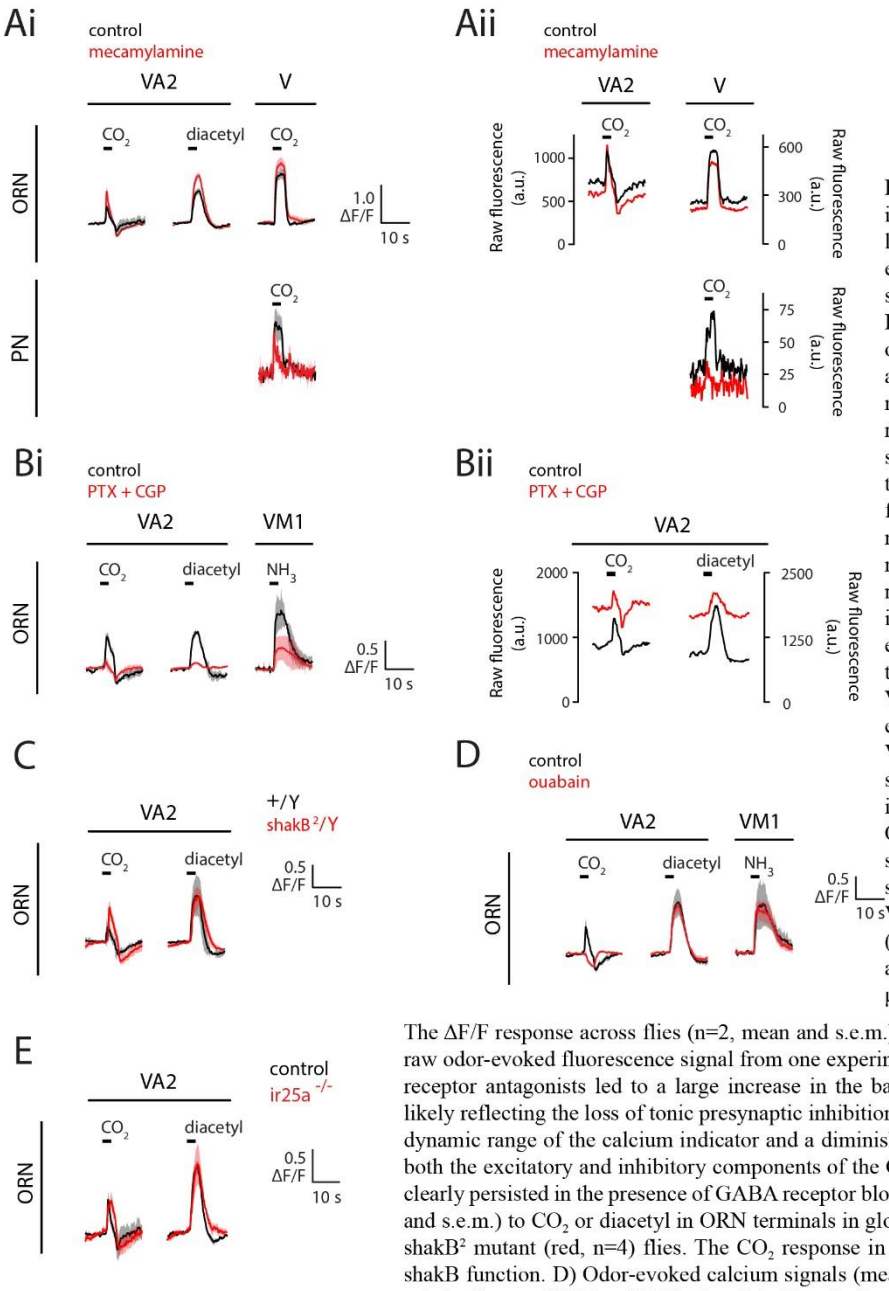

Figure S4: Pharmacological and genetic investigation of the mechanism of lateral signal flow between ORNs (related to Figure 4). A) Odor-evoked calcium signals in either ORN terminals (top) or PN dendrites (bottom) in glomeruli VA2 or V before (black) and after (red) bath application of the cholinergic antagonist mecamylamine (100 μM). The ΔF/F response across flies (n=4, mean and s.e.m.) is shown in Ai, and a representative example of the raw odor-evoked fluorescence signal from one experiment is shown in Aii. Although mecamylamine reduced CO_2-evoked responses in postsynaptic PN dendrites in glomerulus, as expected, both the excitatory and inhibitory components of the CO_2 response in ORN terminals in VA2 were largely unaffected. The small enhancement of some odor responses in VA2 ORNs in mecamylamine could be secondary to a loss of presynaptic inhibition onto ORNs due to blockade of ORN to GABAergic local neuron signaling. B) Odor-evoked calcium signals in ORN terminals in glomeruli VA2 or VM1 before (black) and after (red) bath application of the $GABA_AR$ and $GABA_BR$ antagonists picrotoxin (5 μM) and CGP54626 (50μM), respective. The ΔF/F response across flies (n=2, mean and s.e.m.) is shown in Bi, and an example of the raw odor-evoked fluorescence signal from one experiment is shown in Bii. Wash-in of GABA receptor antagonists led to a large increase in the baseline fluorescence in ORN terminals, likely reflecting the loss of tonic presynaptic inhibition. Although this led to a reduction in the dynamic range of the calcium indicator and a diminishment of the size of all odor responses, both the excitatory and inhibitory components of the CO_2 response in ORN terminals in VA2 clearly persisted in the presence of GABA receptor blockers. C) Odor-evoked responses (mean and s.e.m.) to CO_2 or diacetyl in ORN terminals in glomerulus VA2 in control (black, n=2) or $shakB^2$ mutant (red, n=4) flies. The CO_2 response in VA2 ORNs does not appear to require shakB function. D) Odor-evoked calcium signals (mean and s.e.m., n=4 flies) in ORN terminals in glomeruli VA2 or VM1 before (black) and after (red) bath application of the Na^+/K^+-ATPase inhibitor ouabain (100 μM). Inhibition of the Na^+/K^+-pump resulted in the selective loss of the excitatory component of CO_2 responses in ORN axon terminals in VA2, although the inhibitory component of these responses persisted. In addition, ORN responses to other odors (diacetyl in VA2 and ammonia in VM1) that do not depend on lateral signaling between ORNs were unaffected by application of ouabain. E) CO_2- or diacetyl-evoked responses (mean and s.e.m.) in ORNs in glomerulus VA2 in control (black, n=4) or $ir25a^{-/-}$ (red, n=3) flies. The CO_2-evoked response in VA2 ORNs does not depend on ir25a function. Behavioral genetic experiments indicate that CO_2 attraction depends on the activity of ir25a (van Breugel et al., 2018), which encodes a co-receptor for a subset of the ionotropic class of olfactory receptors (Benton et al., 2009; Silbering et al., 2011). Neither V nor VA2 nor DM1 ORNs are Ir25a-dependent (Benton et al., 2009; Silbering et al., 2011), and CO_2-evoked lateral signals in ORNs in DM1 (data not shown) and VA2 are present in $ir25a^{-/-}$ flies. These results are inconsistent with a role for CO_2-evoked lateral signaling in VA2 and DM1 ORNs in mediating the behavioral attraction to CO_2 described in (van Breugel et al., 2018).

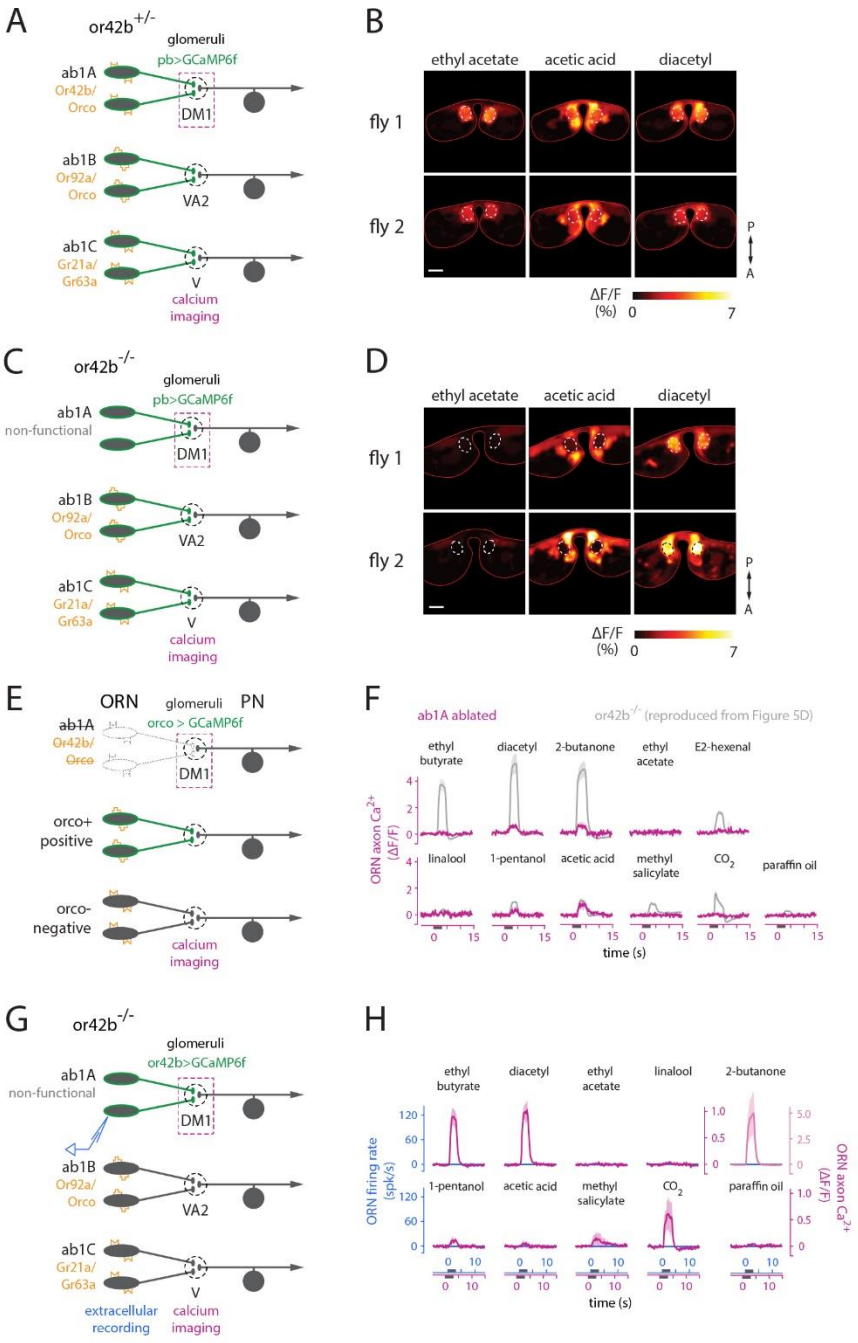

Figure S5: Odors evoke calcium signals in the axon terminals of functionally silent ab1A ORNs lacking odorant receptors (related to Figure 5). A) Schematic of experimental setup. Control recordings in or42b$^{+/-}$ heterozygous flies expressing OpGCaMP6f in all ORNs from the pebbled-gal4 driver. B) Example peak ΔF/F responses in ORN terminals from two individual or42b$^{+/-}$ flies to ethyl acetate (10^{-8}), acetic acid (3%), and diacetyl (10^{-4}) in the imaging plane containing glomerulus DM1 (dashed white line). Note that all three odors evoke responses in ORN terminals in DM1 in the control genotype. Scale bar is 20µm. C) Schematic of experimental setup. Recordings were performed in or42b$^{-/-}$ flies expressing GCaMP6f in all ORNs (from pebbled-gal4). These flies lack a functional odorant receptor in ab1A neurons (which target DM1), thereby abolishing all olfactory transduction and odor-evoked spiking in these ORNs (Figure 5D, blue traces). D) Same as B, but in two example or42b$^{-/-}$ flies. Note the markedly reduced responses of ORN terminals in DM1 to ethyl acetate (10^{-8}) and acetic acid (3%), but the strong response to diacetyl (10^{-4}) (see also Figure 5D). The odor stimuli were presented at the same concentrations as in Figure 5. E) Schematic of experimental setup. ab1A ORNs were ablated by expressing diphtheria toxin under the control of the or42b-gal4 driver. Flies also expressed GCaMP6f in most ORNs under the control of orco-gal4, including in ab1A ORNs if present. F) Time course of changes in fluorescence (ΔF/F, mean and s.e.m.) in glomerulus DM1 in response to a panel of odorants (same as in Figure 5), recorded in the same imaging plane as in Figure 5B, D, F. The analogous responses from or42b$^{-/-}$ flies are overlaid in grey (from Figure 5). the comparative absence of responses when ab1A was ablated (magenta, n=4) demonstrates that responses from the presumed region of interest containing DM1 in this imaging plane are indeed stemming from ab1A ORNs. G) Schematic of experimental setup. The or42b$^{-/-}$ mutation was introduced into flies expressing GCaMP6f selectively in ab1A ORNs under the control of or42b-gal4, allowing unambiguous identification of ab1A axon terminals in a fly where the ab1A ORN lacks an odorant receptor and is functionally silent. H) Comparison of odor-evoked ab1A spiking responses (blue) and the time course of odor-evoked change in fluorescence (ΔF/F, mean and s.e.m.) in ab1A axon terminals (magenta, n = 3). In this fly, ab1A ORNs did not spike in response to odor (blue PSTHs) but ab1A ORN terminals responded robustly to many odors. This result shows that many odors can recruit lateral input to ab1A ORN terminals.

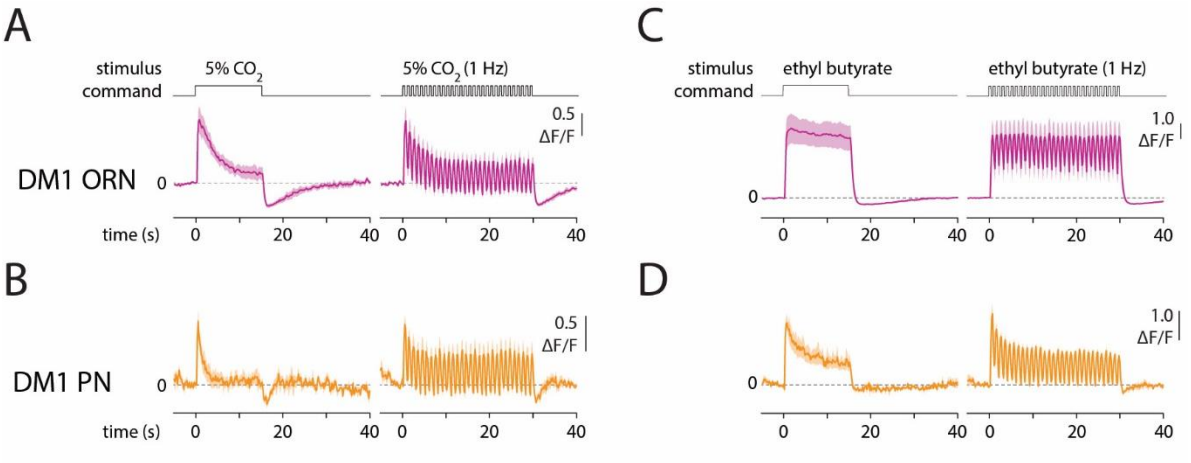

Figure S6. Lateral information flow between ORNs confers odor-specific response dynamics in glomerulus DM1 that are transmitted to downstream PNs (related to Figure 6). A-B) Time course of calcium signals in ORN axon terminals (A, magenta, n = 4 flies) or PN dendrites (B, orange, n = 5-7 flies) in glomerulus DM1 in response to either a sustained 15 s pulse of 10% CO_2 (left) or to a 30 s 1 Hz train of 10% CO_2 pulsed at 50% duty cycle. The top row shows the open-closed state of the odor delivery valve. C-D) Same as panels A-B, but in response to the odor ethyl butyrate (10^{-4}). Calcium signals in DM1 ORN presynaptic terminals adapted rapidly in response to CO2, whereas the signal was more sustained in response to ethyl butyrate. These differences in ORN response dynamics were inherited by downstream PNs.